MSA UNIVERSITY ENGINEERING JOURNAL

Numerical Treatment of MHD Rotating Flow of Nano-Micropolar Fluid with Impact of Temperature-Dependent Heat Generation and Variable Porous Matrix

Hussein AbdAllah Soliman

Department of Basic Science, Engineering Division, an International Academy for Engineering and Media Science
E-mail: Hussein.abdallah.soliman@iaems.edu.eg

Abstract

As the micropolar fluid has an essential rule in cervical flows and the polymer industry, this study looks at the developments of Activation energy and temperature-dependent heat generation effects on the MHD boundary layer flow of nano-micropolar fluid over a porous plate. Viscous and Joule heating, exponentially stretching surface, porous matrix with Darcy expression, and linearized Roseland radiation are considered. The differential equations of the applied system are governed theoretically and solved semi-numerically by the shooting method with the aid of $package\ (ode45)$. The convenient similarity is used to obtain the system of differential equations. Core results show that activation energy improves the rheological characteristics of the thermal boundary layer by moderating the nanoparticle concentration. Furthermore, the distribution of boundary layer velocity is diminished sluggishly as acts of the porous metrics decline the nanofluid velocity. The novelty of the proposed model is the applications of its components which are related to the heat of the Roseland radiative and transpiration cooling system. The rate of the cooling system has a considerable impact on the properties of the final product in polymer technology with the elongation of plastic sheets, thus presenting the final product with some desired appearances.

Keywords: Variable magnetic field, Variable porous matrix, Temperature-dependent heat generation, Arrhenius activation energy, Nano-Micropolar fluid.

1. Introduction

Nowadays, activation energy becomes more significant in scientific research, especially in fluid mechanics. Activation energy is a term proposed for the first time by Svante Arrhenius in 1889 as mentioned in [1]. It means the energy amount articulated in joules necessary to transform molecules in one mole of a reactant from a ground state to a transition state. It can also mean the energy that an atomic system must possess before an emission or chemical reaction can arise. Activation energy transmits the energy required to initiate a reaction. For instance, the activation energy necessary to analyse glucose into pyruvic acid through inhalation is two ATP, etc…. In fluid mechanics, research activation energy appears in many investigations; Salahuddin et al [2] studied the slip velocity and mixed convective heat and mass conditions on boundary layer flow of Carneau fluid with activation energy effect. They found that the Sherwood number has inverse behaviour with activation energy. Over a melting wedge, the Arrhenius energy effect on MHD flow of cross Nano fluid was deliberated by Azama and Abbas [3] . Zeeshan et al [4] discussed the hydromagnetic rotating flow of Nano fluid with Arrhenius energy using RKF45 and stated that the activation energy and chemical reaction parameters have opposite behaviour on the distribution of nanoparticle concentration. In another notification, Bilal et al [5] premeditated the slip conditions and activation energy effects on MHD boundary layer Jeffery fluid. They used the shooting method to find numerical results for skin friction coefficient $(\frac{1}{2}C_{fx}Re_x^{\frac{1}{2}})$. Other manuscripts studied the activation energy effect on fluid flow and its properties see Refs. $[6-10]$.

Micropolar fluids are liquids with a microstructure, which belong to a type of fluids with the tensor non-symmetrical. Especially, micro-polar liquids can signify fluids containing rigid, arbitrarily concerned particles suspended in a viscous medium, where the distortion particles of fluid are unnoticed. Micro-polar fluids were announced for the first time by Eringen [11]. The significance of micropolar fluids in recently published research causes its vital role in lubrication and porous media theories. For instance, Rana et al [12] discussed the Joule heating effect on MHD micropolar fluid over a porous plate. They found that Joule heating and heating mechanisms are undesirably associated with the rate of heat transfer at the plate. Ghadikolaei et al [13] deliberated the MHD boundary layer flow of micropolar nanofluid over a porous plate, and they state that the Hartmann number increases as the Lorentz force reduce the profile of velocity. A study of variable injection/suction on MHD flow of a micropolar fluid with heat generation effect was considered by Goud [14]. Govardhan et al [15] debated the mixed convection MHD flow of micropolar fluid over a stretching sheet. They found that the distribution of microrotation rises near the plate whereas, the opposite behaviour is perceived far away from the plate at high values. More and more studies in the field of micropolar are concerned with fluid mechanics see Refs. $[16-20]$.

In the above-aforementioned studies of micropolar fluid $[11-20]$, the mechanism of Magnetohydrodynamic (MHD) takes all paramount interest. In the present paper, MHD is included in the shared collaboration between the velocity field and electromagnetic lines.

Newly, industries/activities like accelerators, crystal growth, power generators, nuclear physics, etc…the MHD flow of micropolar fluid is considered an essential part of them. Among these studies, Shaha et al [21] premeditated the influence of hall MHD on non-isothermal convective flow. They found that high values of magnetic parameters decrease the value of friction rate. Khader and Sharma [22] studied the thermal radiation effect on MHD micropolar fluid with a heat source and stated that Micropolar fluid angular momentum and velocity profile have opposite behaviour at high values of the magnetic parameter. For more applications and studies of Magnetohydrodynamic see Refs. [23 − 29].

To obtain the results/solutions of the MHD boundary layer flow of micropolar fluid that presented in the current paper, we choose a highly numerical technique named by shooting method combination with Runge-Kutta method (ODE45). Generally, in numerical analysis, the shooting method is considered a highly constructive technique that is used to solve the boundary value problem by dropping it to an initial value problem. It includes finding solutions to the initial value problem of various initial conditions until one finds the solution which also satisfies the boundary conditions of the boundary value problem. The shooting method is proposed firstly by Merle 1988 [30], who find the solution to nonlinear Dirac equations. In early time, Hasanuzzaman et al [**31**] use the shooting technique to find solutions to the transpiration effect on the MHD boundary layer flow problem. Lanjwani et al [32] studied the MHD Laminar Boundary Layer Flow of Casson Nanofluid using the shooting method. Many authors and investigators use the shooting method to obtain solutions to various boundary value problems, see Refs. [33 − 37].

The main aim of this study is to make a new suggestion for a temperature-dependent heat generation study on the MHD boundary layer flow of micropolar fluid using a highly accurate technique called the shooting method. The solution of the proposed model is offered in different two cases, the first in the case of viscous fluid ($K = 0$), and the other in the micropolar fluid case ($K = 1$). Results for velocities gradients, temperature, and concentration distributions are offered in different mentioned cases. The novelty of the proposed model is the applications of its components which are related to the heat of the Roseland radiative and transpiration cooling system. The rate of the cooling system has a considerable impact on the properties of the final product in polymer technology with the elongation of plastic sheets, thus presenting the final product with some desired appearances. All presented results are obtained using the shooting method.

2. Mathematical Formulations

Heat generation dependent temperature and Rosseland thermal radiation effects on the two-dimensional boundary layer of micropolar nanofluid with the elongating sheet are considered. $x-$ axis and $y-$ axis are along the stretchable and vertical plates, respectively. The velocity of the sheet elongated and was supposed as $u_w = ae^{x/l}$ where $a > 0$. Magnetic field $B = B_0 e^{x/2l}$ is supposed to be variable. The description of the fluid model is basically as follows, see Rana et al [12]:

$$\frac{\partial u'}{\partial x'} + \frac{\partial v'}{\partial y'} = 0 \tag{1}$$

The equation of Conservation of linear momentum

$$u'\frac{\partial u'}{\partial x'}+v'\frac{\partial u'}{\partial y'}=\left(\nu+\frac{\kappa}{\rho}\right)\frac{\partial^2 u'}{\partial y'^2}+\frac{\kappa}{\rho}\frac{\partial N'}{\partial y'}-\left(\frac{\sigma B^2}{\rho}+\frac{\nu}{KP^*}\right)u' \tag{2}$$

The equation of microrotation conservation:

$$u'\frac{\partial N'}{\partial x'}+v\frac{\partial N'}{\partial y'}=\frac{\gamma}{\rho j}\frac{\partial^2 N'}{\partial y'^2}-\frac{\kappa}{\rho j}\left(2N+\frac{\partial u'}{\partial y'}\right) \tag{3}$$

The equation of energy conservation combined with model of Buongiorno:

$$u'\frac{\partial T'}{\partial x'}+v'\frac{\partial T'}{\partial y'}=\left(\alpha^*+\frac{16\sigma_1 T_\infty^3}{m_1(\rho C_p)}\right)\frac{\partial^2 T'}{\partial y'^2}+\tau\left[D_B\frac{\partial C'}{\partial y'}\frac{\partial T'}{\partial y'}+\frac{D_{T'}}{T'_\infty}\left(\frac{\partial T'}{\partial y'}\right)^2\right]+\frac{(\mu+\kappa)}{\rho C'_p}\left(\frac{\partial u'}{\partial y'}\right)^2+$$

$$\frac{\sigma B^2}{\rho C_p}u'^2+\frac{Q}{\rho C_p}(T'-T'_\infty) \tag{4}$$

The nanoparticles conservation

$$u'\frac{\partial C'}{\partial x'}+v'\frac{\partial C'}{\partial y'}=D_B\frac{\partial^2 C'}{\partial y'^2}+\frac{D_{T'}}{T'_\infty}\frac{\partial^2 T'}{\partial y'^2}-K_r^2(C'-C'_\infty)\left(\frac{T'}{T'_\infty}\right)^n e^{\left(\frac{-E'_a}{K_B T'}\right)} \tag{5}$$

The chosen/appropriate boundary conditions are described as follows:

$$u'=u'_w(x)=ae^{\frac{x}{\iota}},v'=v'_w(x)=-v'_0 e^{\frac{x}{2\iota}},N'-m\frac{\partial u'}{\partial y'},T'=T'_w,C'=C'_w \text{ at } y=0 \tag{6}$$

$$u'\to 0,N'\to 0,\ T'\to T'_\infty, \text{ and } C'\to C'_\infty\ as\ \ y\to\infty \tag{7}$$

Where $(u',\ v')$ and m are the velocities along x and y direction respectively, and the condition parameter, which $0\le m\le 1$. In the case of $m=0, m=0.5$ and $m=1$ are denotes the strong concentration, weak concentration, and turbulent flows, correspondingly (see [**17**]), $K_{P^*}=K_{P0}e^{\frac{-x}{\iota}}$ is the porous matrix, $Q=Q_0e^{\frac{x}{\iota}}$ is the variable heat sink, and $v_w=-v_0e^{\frac{x}{2\iota}}$ is the suction/injection, the coefficients velocity with B_0, Kp_0, Q_0 and v_0 are constants. Supposing that γ is given by

$$\gamma=\left(\mu+\frac{\kappa}{2}\right)\mathrm{j}=\mu\left(1+\frac{K}{2}\right)j \tag{8}$$

Where $K=\frac{\kappa}{\mu}$ is the material parameter and the microinertia per unit mass is $j=\frac{2l\nu e^{-x/l}}{a}$

The appropriate transformations are proposed:

$$u=ae^{\frac{x}{\iota}}f'(\eta),v=-\sqrt{\frac{a\nu}{2\iota}}e^{\frac{x}{2\iota}}\{f(\eta)+nf'(\eta)\},N=ae^{\frac{3x}{2\iota}}\sqrt{\frac{a}{2\nu\iota}}g(\eta)\quad,\quad \eta=y\sqrt{\frac{a}{2\nu\iota}}e^{\frac{x}{2\iota}}$$

$$\theta(\eta)=\frac{T'-T'_\infty}{T'_w-T'_\infty}\quad\text{and}\quad\phi(\eta)=\frac{C'-C'_\infty}{C'-C'_\infty}. \tag{9}$$

Here η is the similarity variable, $f(\eta)$ is the non-dimensional stream function, $f'(\eta)$ axial velocity, $\theta(\eta)$ is the temperature, $g(\eta)$ is the rotation of the micropolar particles, and $\phi(\eta)$ nanoparticles volume fraction, correspondingly. The governing system of differential

equations are transformed/ non-dimensional as follows.

$$(1+K)f''' + 2f'^2 + ff'' - Kg' - \left(\frac{1}{K_p} + M\right)f' = 0, \tag{10}$$

$$\left(\frac{K}{2} + 1\right)g'' - 3f'g + fg' - K(2g + f'') = 0 \tag{11}$$

$$\frac{(1+R_d)\theta''}{P_r} + Nb\ \theta'\phi' + Nt\ \theta'^2 + S\theta + E_c\ (1+K)f''^2 + f\theta' + ME_c\ f'^2 = 0, \tag{12}$$

$$\phi'' + L_e P_r f\phi' + \frac{N_t}{N_b}\theta'' - P_r L_e \sigma(1+\delta\ \theta)^n e^{\left(\frac{-E}{1+\delta\ \theta(\eta)}\right)}\phi = 0. \tag{13}$$

With transformed boundary conditions

$$f(0) = \lambda,\ f'(0) = 1,\ g(0) = -mf'',\ \theta(0) = 1 \text{ and } \phi(0) = 1, \tag{14}$$

$$f'(\infty) = 0,\ g(\infty) = 0,\ \ \theta(\infty) = 0, \text{ and } \phi(\infty) = 0. \tag{15}$$

Where $M = \frac{2\sigma B_0^2\, \iota}{\rho\ a}$ is the Hartmann number, $K_p = \frac{2\ \iota\upsilon}{a\ K\ p_0}$ is the porous parameter $P_r = \frac{\upsilon}{\alpha}$ is the Prandtl number, $R_d = \frac{16\ \sigma^*\ T_\infty^3}{3\ k\ k^*}$ is the radiation parametetr $E_c = \frac{u_w^2}{c_p\ (T_{w-}\ T_\infty)}$ is the Eckert number, $S = \frac{2\iota Q_0}{a\rho C_p}$,is the heat source factor $Nb = \frac{\tau D_B\ (C_{w-}\ C_\infty)}{\upsilon}$ is the Brownian motion parameter, $Nt = \frac{\tau D_T\ (T_{w-}\ T_\infty)}{\upsilon T_\infty}$ is the thermophoresis parameter, $\lambda = \frac{v_0}{\sqrt{\frac{a\upsilon}{2\iota}}}$ is the transpiration parameter, $\sigma = \frac{k_r^2}{a}$ is the chemical reaction species, $L_e = \frac{\nu}{D_B}$ *i*s the Lewis number, $\delta = \frac{T_w' - T_\infty'}{T_\infty'}$ is the temperature difference parameter and $E = \frac{E_a}{K_B T'}$ is the Activation energy.

3. Method of Solution

Numerical solutions of the ordinary differential Eqs. (10-13) subject to Neumann boundary conditions (15-16) are obtained using classical Runge–Kutta method with shooting techniques and MATLAB package (ode45). The set of coupled nonlinear ordinary differential equations along with boundary conditions have been reduced to a system of simultaneous equations of the first order for the unknowns following the method of superposition in Na [38]. Equations (10-13) can be written as follows:

$$z_1' = z_2, \tag{16}$$

$$z_2' = z_3, \tag{17}$$

$$z_3' = \frac{-2(z_2)^2 - z_1 z_3 + Kz_4 + \left(\frac{1}{K_p} + M\right)z_2}{(1+K)} \tag{18}$$

$$z_4' = z_5, \tag{19}$$

$$z_5' = \frac{3z_2z_4 - z_1z_5 + K(2z_4 + z_3)}{\left(\frac{K}{2} + 1\right)} \tag{20}$$

$$z_6' = z_7, \tag{21}$$

$$z_7' = \frac{-Nb\, z_7z_9 - Nt\,(z_7)^2 - S\, z_6 + E_c\,(1+K)f''^2 - z_1z_7 - ME_c\,(z_2)^2}{\frac{(1+R_d)}{P_r}} \tag{22}$$

$$z_8' = z_9, \tag{23}$$

$$z_9' = -L_eP_rz_1\, z_9 - \frac{N_t}{N_b}z_7' + P_rL_e\sigma(1+\delta\ z_6)^n e^{\left(\frac{-E}{1+\delta z_6}\right)}z_8 \tag{24}$$

Where z_1=f, z_2=f′, z_3= f′′, z_4=g, z_5=g′, z_6= θ, z_7= θ′, z_8= ϕ and z_9=ϕ′ and prime denotes a derivative of the function with respect to η. The corresponding boundary conditions will become:

$z_1(0)= \lambda$, $z_2(0)=1$, $z_3(0)=i_1$, $z_4(0)=-mz_3$, $z_5(0)= i_2$, $z_6(0)=1$, $z_7(0)= i_3$, $z_8(0)=1$ and $z_9(0)= i_4$ (20)

$z_2(\infty)=0$, $z_4(\infty)=0$, $z_6(\infty)=0$ and $z_8(\infty)=0$. (21)

Wherei_1, i_2, i_3 and i_4 are a priori unknowns that must be resolved using shooting technique as part of the solution. (Ode45) integrates the system of differential Eqs. (16-24) with suitable guess values for initial conditions i_1, i_2, i_3 and i_4. The procedure is repeated with another value of η∞ until two successive values of i_1, i_2, i_3 and i_4 are differ only by the desired accuracy. We have compared the calculated values of f′, g, θ, and ϕ at $\eta = 10$ with the given boundary conditions and adjusted the estimated values of i_1, i_2, i_3 and i_4 to give a better approximation. The step size is reduced until to get the required accuracy.

4. Analysis of results

This section introduce a graphical results of physical parameters of interest like porous parameter K_p, activation energy E, heat source factor S, radiation parameter R_d, transpiration parameter λ, Hartmann number M, and chemical reaction species σ on the distributions of velocity $f'(\eta)$, microrotation $g(\eta)$, temperature $\theta(\eta)$ and nanoparticle concentration $\varphi(\eta)$ through Figs. 1-14. Polynomials of different cases of temperature and concentration profiles are constructed numerically at different cases of viscous fluid $K = 0$ and Micro polar fluid $K = 1$ as appendix in the last part of this section. It's worth mention that the standard values of parameters for all obtained figures is $P_r = 1, N_b = 0.2, M = 0.8, \delta = 0.1, N_t = 0.2,\ E = 0.1, \sigma = 0.4, m = 0.1, \gamma = 0.1, R_d = 0.3, Le = 0.1, S = 0.5, \lambda = 0.6 K_p = 0.4$.

It's depicted from Figs. 1-2 that the magnetism/Hartmann parameter M and transpiration parameter λ are decreasing function in velocity distribution. The Lorentz force instigated by the applied magnetic field which diminishes the velocity. Physically, the collaboration of the magnetism in an electrically conductive fluid offerings a delaying body force, recognized as the Lorentz force that decelerates the fluid velocity see Refs. [12, 17]. In additions, the fluid is slurped from the system surface, it reasons a resistive force; accordingly, the distributed velocity declines for high values of transpiration parameter. Various values of porous matrix parameter K_p is visualized sketchily through Fig. 3. High values of K_p make the velocity of fluid particle increases which contrary to expected.

It's portrayed from Figs. 4-5 that the micro rotation field $g(\eta)$ has two opposite behavior in case of high values of Hartmann number and porosity. In case of viscous fluid $K = 0$ the microrotation filed has a high values on the axis than found in the case of micropolar fluid $K = 1$. It's showed from Fig. 6 that the high values of transpiration parameter λ increase the micro rotation field $(g(\eta))$ near the surface in the region $\eta < 0.35$), whilst the reverse behaviour is seeming near the stretching surface in the region $\eta > 0.35$.

It's seen from Fig. 7 that the high values heat sink parameter $S > 0$ give the particle more energy which produce an additional heat because of viscous heating and heat source mechanisms. Also, Figs. 8-9 shows that the high values of radiation R_d and transpiration λ parameters are decrease the temperature distribution. Physically, the rate of the cooling system has a considerable impact on the properties of the final product in polymer technology with the elongation of plastic sheets, thus presenting the final product with some desired appearances.

It's represented from Figs. 10-12 that the thermal Roseland radiation R_d, activation parameter E , and transpiration parameter λ are increasing function in nanoparticle concentration. Physically that's infers a moderately strong concentration of microelements which present on the surface at high values of R_d, λ andE. Heat sink parameter S and chemical reaction σ are studied contrary with nanoparticle concentration through Figs. 13-14. It's portrayed the high values of S and σ decline the distribution of nanoparticle concentration. Behaviour of chemical reaction species has more sight features on the volume fraction. Eventually, the nanoparticles thermo-migration eases the growth of nanoparticle concentration boundary layer mechanism.

Table 1 is numerically computed to assure the accuracy of shooting method at the standard values of parameters and zero activation energy and $R_d = 0$. Comparison has been made between the prior results and the nearest published results by Rana et al [12] for skin friction coefficient $-f''(0)$. It's observed from Table 1 that the shooting technique is a good algorithm for obtaining the numerical results of boundary layer flow of non-Newtonian fluid models.

Table 1: comparison of skin friction coefficient $-f''(0)$ at zero activation energy and $R_d = 0$.

M	K_p	λ	K	σ	$-f''(0)$ RKSM Rana et al **[12]**	$-f''(0)$ present results
0	100	0	0	0	1.286094	1.286654
0.5	100	0	0	0	1.469904	1.469980
1	100	0	0	0	1.632263	1.632985
1	10	0	0	0	1.659750	1.659721
1	1	0	0	0	1.912620	1.912645
1	1	0.1	0	0	1.961740	1.961764
1	1	0.3	0	0	2.063999	2.063987
1	1	0.3	0.5	0	1.649661	1.649623
1	1	0.3	1	0	1.400387	1.400371

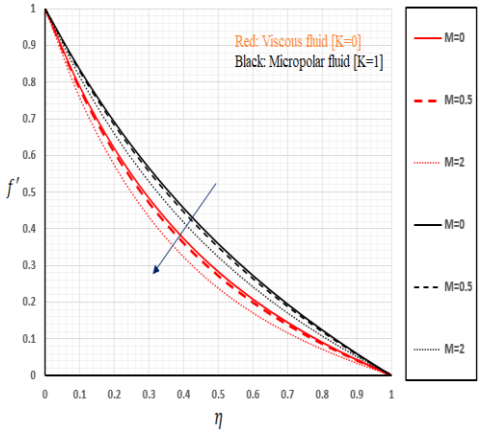

Fig. 1: Velocity distributions $f'(\eta)$ versus M

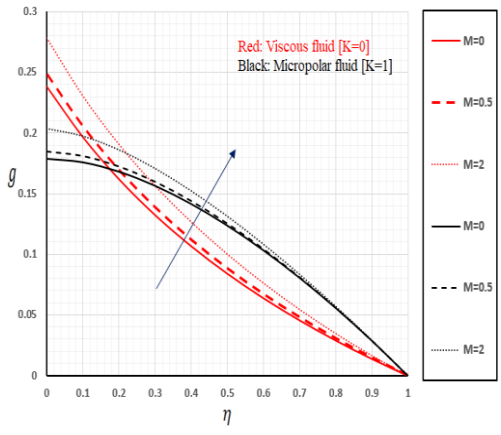

Fig. 4: Microrotation distributions $g(\eta)$ versus M

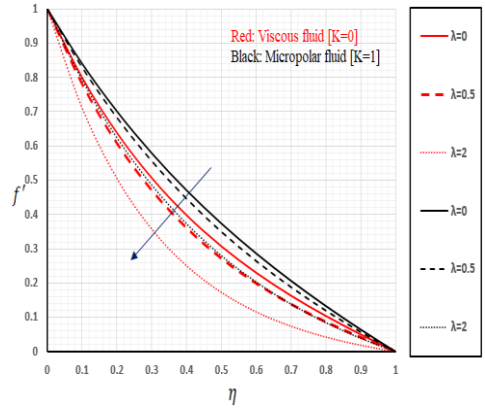

Fig. 3: Velocity distributions $f'(\eta)$ versus K_p

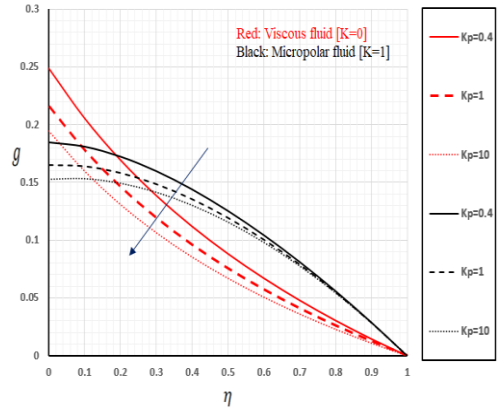

Fig. 5: Microrotation distributions $g(\eta)$ versus K_p

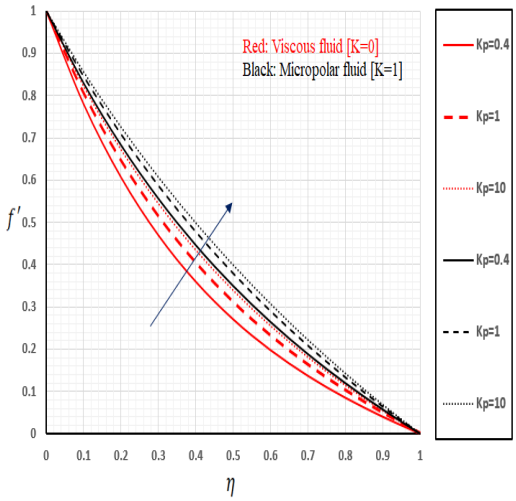

Fig. 2: Velocity distributions $f'(\eta)$ versus K_p

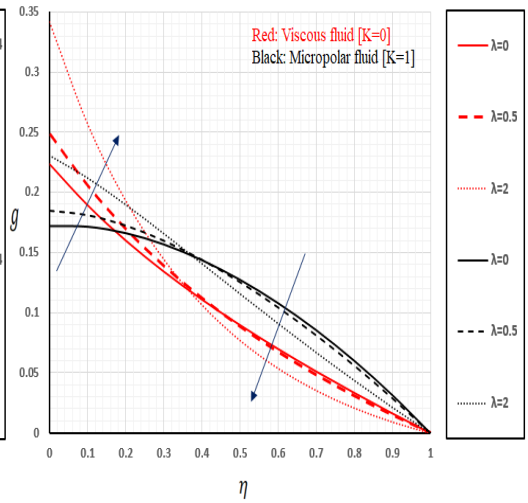

Fig. 6: Microrotation distributions $g(\eta)$ versus λ

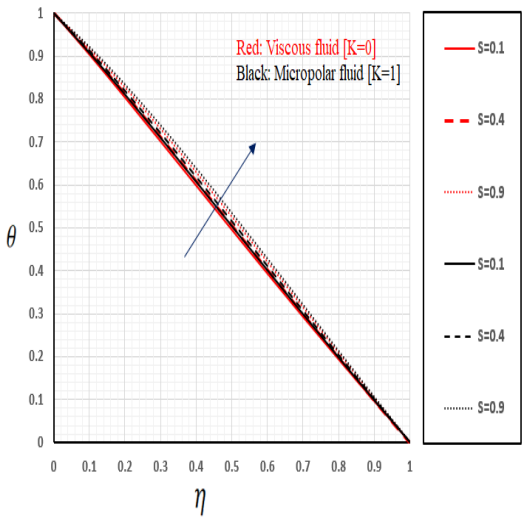

Fig. 7: Temperature distributions $\theta(\eta)$ versus S

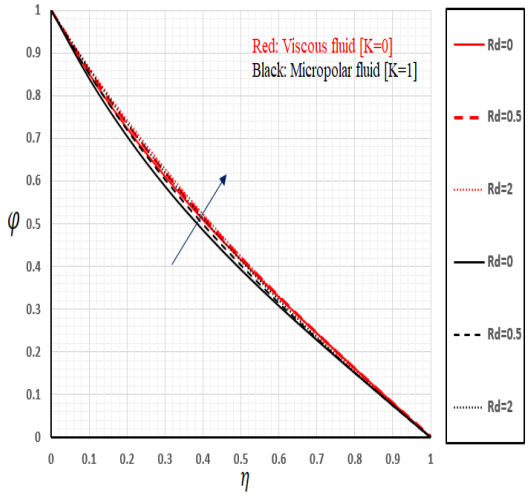

Fig. 10: Concentration distributions $\varphi(\eta)$ versus R_d

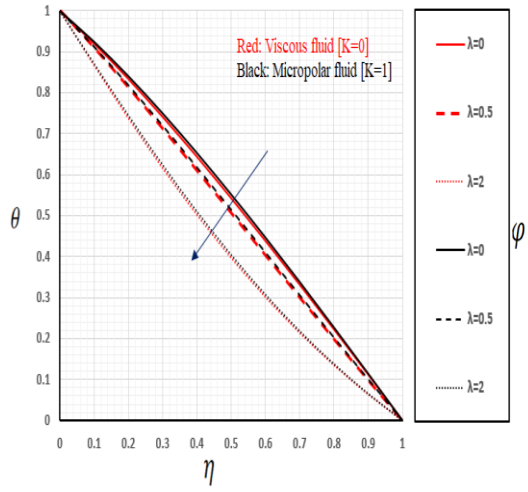

Fig. 8: Temperature distributions θ(η) versus λ

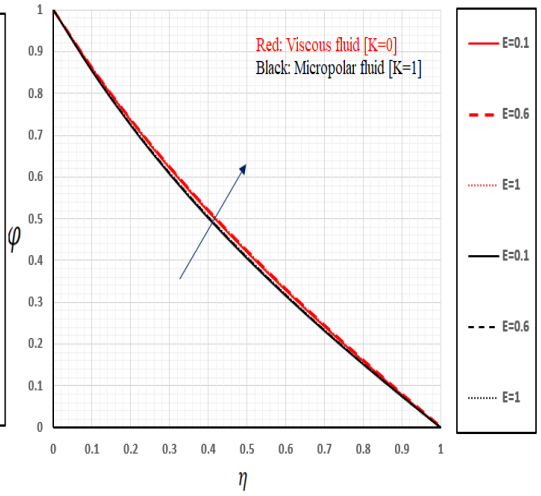

Fig. 11: Concentration distributions φ(η) versus E

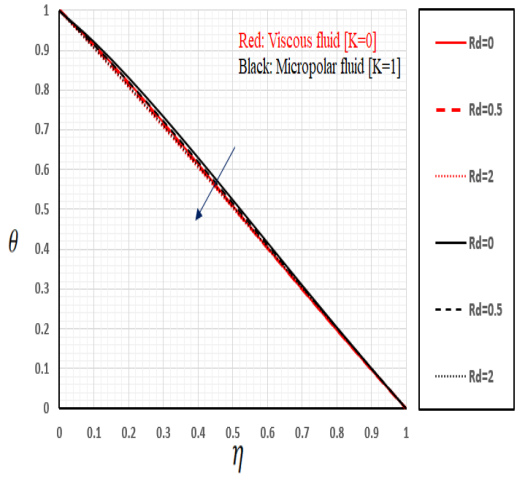

Fig. 9: Temperature distributions θ(η) versus R_d

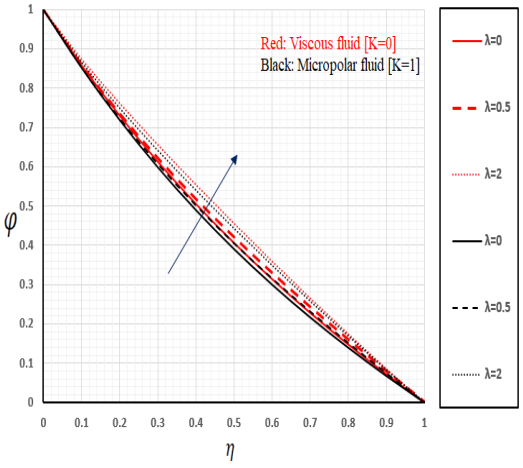

Fig. 12: Concentration distributions φ(η) versus λ

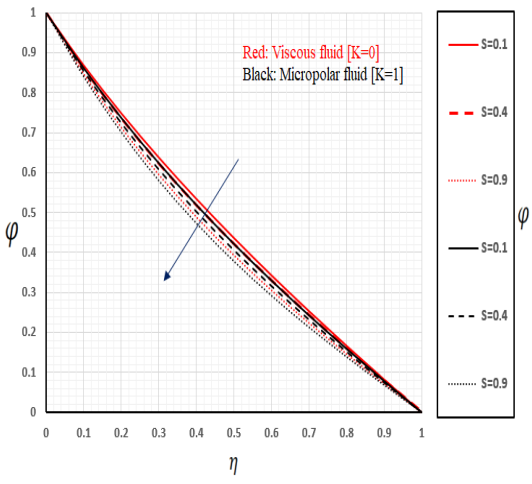

Fig. 13: Concentration distributions φ(η) versus S

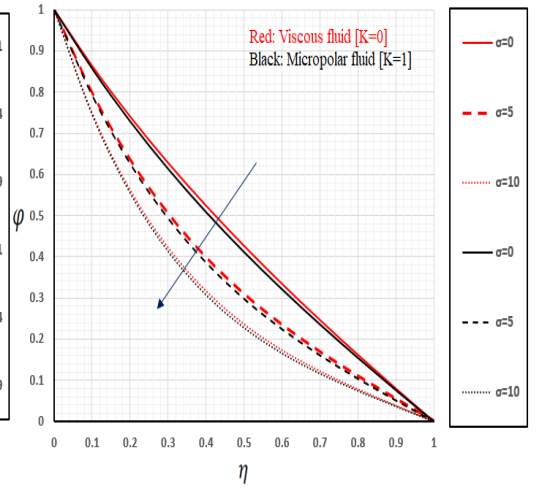

Fig. 14: Concentration distributions φ(η) versus σ

Appendix

The polynomials of nanoparticle concentration versus values chemical reaction species.

$\sigma = 10, K = 0.$

$$\varphi = 1 - 2.8955 * x + 4.2572 * x^2 - 4.1409 * x^3 + 2.7758 * x^4 - 1.366 * x^5 + 0.44597 * x^6 - 0.071651 * x^7 - 0.011897 * x^8 + 0.0084228 * x^9 - 0.0013481 * x^{10}.$$

$\sigma = 10, K = 1$

$$\varphi = 1 - 2.947 * x + 4.3014 * x^2 - 3.9552 * x^3 + 2.2815 * x^4 - 0.73552 * x^5 - 0.088539 * x^6 + 0.25834 * x^7 - 0.15873 * x^8 + 0.050919 * x^9 - 0.0072986 * x^{10}.$$

The polynomials of temperature versus values chemical reaction species.

σ=10, K=0

$$\theta = 1 - 0.86188 * x - 0.49841 * x^2 + 0.69668 * x^3 - 0.62599 * x^4 + 0.52515 * x^5 - 0.40534 * x^6 + 0.26664 * x^7 - 0.13335 * x^8 + 0.043038 * x^9 - 0.0065364 * x^{10},$$

σ=10, K=1

$$\theta = 1 - 0.81987 * x - 0.52196 * x^2 + 0.54096 * x^3 - 0.26778 * x^4 + 0.073163 * x^5 + 0.0066335 * x^6 - 0.017654 * x^7 + 0.007934 * x^8 - 0.0014699 * x^9 + 4.6177e^{-5} * x^{10}$$

5. Conclusion

This paper looks at the developments of porous matrix and temperature-dependent heat generation effects on MHD boundary layer flow of nano-micropolar fluid over a porous plate. Viscous and Joule heating, exponentially stretching surface, with Darcy expression, and linearized Roseland radiation are considered. The differential equations of the applied system are governed theoretically and solved semi-numerically by shooting method. The main points extracted through these studies can be as follows:

- Shooting method obtain the solution of boundary layer problem without linearization, perturbation or restrictive assumptions.
- Good agreement between the prior results and existing published results by Rana et al 2021.
- The present system of equations can easily use in polymer technology with the elongation of plastic sheets.
- The rate of heat transport rate reduces at high values of applied magnetic field at the plate.
- The nanoparticles thermo-migration eases the growth of nanoparticle concentration boundary layer mechanism.
- Transpiration parameter has a dual role phenomenon on the micro rotation distribution.

References

[1] N. V. Ganesh, R. Kalaivanan, Q. M. Al-Mdallal and K. Reena, Buoyancy driven second grade nano boundary layers over a catalytic surface with reaction rate, heat of reaction and activation energy at boundary, Case Studies in Thermal Engineering, 28, 2021, 101346.

[2] T. Salahuddin, M. Awais and Z. Salleh, A flow study of Carreau fluid near the boundary layer region of paraboloid surface with viscous dissipation and variable fluid properties, journal of materials research and technology, 14 (2021) 901-909.

[3] M. Azama and Z. Abbasb, Recent progress in Arrhenius activation energy for radiative heat transport of cross nanofluid Q2Q6 over a melting wedge, Propulsion and Power Research, 10 (2021)1-13.

[4] A. Zeeshan, O. U. Mehmood, F. Mabood and F. Alzahrani, Numerical analysis of hydromagnetic transport of Casson nanofluid over permeable linearly stretched cylinder with Arrhenius activation energy, International Communications in Heat and Mass Transfer, 130 (2022) 105736.

[5] S. Bilal, S.U. Mamatha, C. S. K. Raju, B. M. Rao, M. Y. Malik and A. Akgul, Dynamics of chemically reactive Jeffery fluid embedded in permeable media along with influence of magnetic field on associated boundary layers under multiple slip conditions, Results in Physics, 28 (2021) 104558.

[6] I. Ullah, M. Alghamdi, W. Xia, S. I, Shah and H. Khan, Activation energy effect on the magnetized-nanofluid flow in a rotating system considering the exponential heat source, International Communications in Heat and Mass Transfer, 128 (2021) 105578.

[7] U. Ahmed, N. Chakraborty and M. Klein, Influence of thermal wall boundary condition on scalar statistics during flame-wall interaction of premixed combustion in turbulent boundary layers, International Journal of Heat and Fluid Flow 92 (2021) 108881.

[8] D. Lu, M. Ramzan, S. Ahmad, J. D. Chung, U. Farooq, Upshot of binary chemical reaction and activation energy on carbon nanotubes with Cattaneo–Christov heat flux and buoyancy effects, Physics of Fluids, 29, (2017),123103.

[9] A. Zaib A, M. M. Rashidi, A. J. Chamkha and K. Bhattacharyya. Numerical solution of second law analysis for MHD Casson nanofluid past a wedge with activation energy and binary chemical reaction. International Journal of Numerical Methods for Heat & Fluid Flow, 27, (2017) 2816–2834.

[10] G. K. Ramesh, S. A. Shehzad, T. Hayat and A. Alsaedi, Activation energy and chemical reaction in Maxwell magneto-nanoliquid with passive control of nanoparticle volume fraction, Journal of the Brazilian Society of Mechanical Sciences and Engineering, 40, (2018)422.

[11] C. A. Eringen, Theory of thermo-micro fluids, Journal of Mathematical Analysis and Applications38 (1972) 480–496.

[12] P. Rana, B. Mahanthesh, K. S. Nisar, K. Swain and M. Devi, Boundary layer flow of magneto-nanomicropolar liquid over an exponentially elongated porous plate with Joule heating and viscous heating: a numerical study, Arabian Journal for Science and Engineering, 46 (2021) 12405–12415.

[13] S. S. Ghadikolaei, Kh. Hosseinzadeh, M. Hatami and D. D. Ganji, MHD boundary layer analysis for micropolar dusty fluid containing Hybrid nanoparticles (Cu Al2O3) over a porous medium, Journal of Molecular Liquids, 268 (2018) 813–823.

[14] B. S. Goud, Heat generation/absorption influence on steady stretched permeable surface on MHD flow of a micropolar fluid through a porous medium in the presence of variable suction/injection, International Journal of Thermofluids, 7–8, (2020) 100044.

[15] K. Govardhan, G. Nagaraju, K. Kaladhar and M. Balasiddulu, MHD and radiation effects on mixed convection unsteady flow of microploar fluid over a stretching sheet, Procedia Computer Science 57 (2015) 65 – 76.

[16] Srinivasacharya, D. and Himabindu, K., 2017, "Analysis of Entropy Generation Due to Fluid Flow in a Rectangular Duct Subjected to Slip and Convective Boundary Conditions", J. Heat Transfer, 139(7): 072003.

[17] A. Ishak, Thermal boundary layer flow over a stretching sheet in a micropolar fluid with radiation effect. Meccanica, 45 (2010) 367–373.

[18] Srinivasacharya, D. and Shiferaw, M., 2013, "Cross Diffusion effects on chemically reacting magnetohydro -dynamic micropolar fluid between concentric cylinders", J. Heat Transfer, 135(12): 122003.

[19] Khalid, I. K., Mokhtar, N. F. M. and Arifin, N. M., 2013, "Uniform solution on the combined effect of magnetic field and internal heat generation on Rayleigh–Bénard convection in micropolar fluid" J. Heat Transfer, 135(10): 102502.

[20] Srinivasacharya, D. and RamReddy, Ch., 2011, "Effect of Double Stratification on Free Convection in a Micropolar Fluid", J. Heat Transfer, 133(12): 122502.

[21] Z. Shaha, M. Shutaywi, A. Dawar, P. Kumamd, P. Thounthongf and S. Islam, Impact of Cattaneo-Christov heat flux on non-isothermal convective micropolar fluid flow in a hall MHD generator system, Journal of Materials Research and Technology, 9(3) (2020) 5452–5462.

[22] M. M. Khader, R. P. Sharm, Evaluating the unsteady MHD micropolar fluid flow past stretching/ shirking sheet with heat source and thermal radiation: Implementing fourth order predictor–corrector FDM, Mathematics and Computers in Simulation, 181 (2021) 333–350.

[23] R. S. Tripathy, G. C. Dash, S. R. Mishra and M. M. Hoque, Numerical analysis of hydromagnetic micropolar fluid along a stretching sheet embedded in porous medium with non-uniform heat source and chemical reaction, Engineering Science and Technology, an International Journal, 19 (2016) 1573–1581.

[24] Rahman, M. M. and Sattar, M. A., 2006, "Magnetohydrodynamic Convective Flow of a Micropolar Fluid Past a Continuously Moving Vertical Porous Plate in the Presence of Heat Generation/Absorption", J. Heat Transfer, 128(2): 142–152.

[25] L. A. Lund, Magnetohydrodynamic (MHD) flow of micropolar fluid with effects of viscous dissipation and Joule heating over an exponential shrinking sheet. Symmetry, 12, 142–158 (2020)

[26] G. Nagaraju, Srinivas Jangili, J. V. Ramana Murthy, Bég, O. A. and Kadir, A.,

[27] S. U. Rehman, A. Mariam, A. Ullah, M. I. Asjad, M. Y. Bajuri, B. A. Pansera and A. Ahmadian, Numerical computation of buoyancy and radiation effects on MHD micropolar nanofluid flow over a stretching/shrinking sheet with heat source, Case Studies in Thermal Engineering, 25,(2021)

[28] S. S. Ghadikolaei, K. Hosseinzadeh, D. D. Ganji and B. Jafari, Nonlinear thermal

radiation effect on magneto Casson nanofluid flow with Joule heating effect over an inclined porous stretching sheet. Case Studies in Thermal Engineering, 12 (2018)176–187.

[29] S. R. Mishra, M. M. Hoque, B. Mohanty and N. N. Anika, Heat transfer effect on MHD flow of a micropolar fluid through porous medium with uniform heat source and radiation. Nonlinear Engineering, 8 (2019) 65–73.

[30] F. Merle, Existence of stationary states for nonlinear Dirac equations, Journal of Differential Equations, 74 (1988), 50–68.

[31] M. D. Hasanuzzaman, M. D. A. Kabir and M. D. T. Ahmed, Transpiration effect on unsteady natural convection boundary layer flow around a vertical slender body, Results in Engineering, 12 (2021)100293.

[32] H. B. Lanjwani, M. S.Chandio, M. I. Anwar, S. A. Shehzad and M. Izadi, MHD Laminar Boundary Layer Flow of Radiative Fe-Casson Nanofluid: Stability Analysis of Dual Solutions, Chinese Journal of Physics, (2021), In Press.

[33] L. Charroyer, O. Chiello and J.J. Sinou, Estimation of self-sustained vibration for a finite element brake model based on the shooting method with a reduced basis approximation of initial conditions, Journal of Sound and Vibration 468 (2020) 115050.

[34] S. Florian and C. Damien, Geometrically exact static 3D Cosserat rods problem solved using a shooting method, International Journal of Non-Linear Mechanics, 119 (2020) 103330.

[35] I. K. Argyros, J. Ceballos, D. González and J. M. Gutiérrez, Extending the applicability of Newton's method for a class of boundary value problems using the shooting method, Applied Mathematics and Computation 384 (2020) 125378.

[36] P. B. Madabhushi and T. A. Adams, On the application of shooting method for determining semicontinuous distillation limit cycles, Chemical Engineering Research and Design, 160 (2020) 370-382.

[37] J. Zhang, R. Zhang and L. Yang, Topographic solitary waves by the shooting method and Fourier spectral method, Results in Physics, 16 (2020) 102944.

[38] NA, T. (1979). Computational methods in engineering boundary value problems(Book). New York, Academic Press, Inc. (Mathematics in Science and Engineering., 145.